Large $|\eta|$ approach to single field inflation

Gianmassimo Tasinato[*]

Dipartimento di Fisica e Astronomia, Università di Bologna, Bologna 37200, Italia and Physics Department, Swansea University, Swansea SA28PP, United Kingdom

(Received 1 June 2023; accepted 4 August 2023; published 23 August 2023)

Single field models of inflation capable of producing primordial black holes usually require a significant departure from the standard, perturbative slow-roll regime. In fact, in many of these scenarios, the size of the slow-roll parameter $|\eta|$ becomes larger than one during a short phase of inflationary evolution. In order to develop an analytical control on these systems, we explore the limit of $|\eta|$ large, and promote $1/|\eta|$ to a small quantity to be used for perturbative expansions. Formulas simplify, and we obtain analytic expressions for the two and three point functions of curvature fluctuations, which share some of the features found in realistic inflationary models generating primordial black holes. We study one-loop corrections in this framework: we discuss criteria for adsorbing ultraviolet divergences into the available parameters, leaving log-enhanced infrared contributions of controllable size.

DOI: 10.1103/PhysRevD.108.043526

I. INTRODUCTION AND CONCLUSIONS

Identifying the nature of dark matter is one of the most challenging open problems in cosmology [1]. A fascinating possibility is that dark matter is made of primordial black holes (PBH) [2–5], forming from the collapse of high density fluctuations produced during cosmic inflation: see e.g. [6–12] for reviews. In order for producing PBH, the size of the inflationary curvature fluctuation spectrum needs to increase by around seven orders of magnitude, from large to small scales. This condition is not possible to achieve within a controlled slow-roll expansion in single-field inflation [13]: a departure from the standard slow-roll conditions is needed. In several single-field realizations of PBH scenarios, the size $|\eta|$ of the second slow-roll parameter becomes larger than one during a brief phase of nonslow-roll evolution (from now on, NSR). Such brief NSR era should last few e-folds $\Delta N_{\rm NSR}$ of expansion. Examples are ultra-slow-roll models [14–16], where $\eta = -6$, and constant roll models [17–19], where $|\eta|$ can be larger or smaller than 6, depending on the properties of the inflationary potential. In these cases, the evolution of fluctuations challenges analytical investigations, since the slow-roll expansion breaks down. Wands duality [20] can be of help in the ultraslow-roll case, but still care is needed in connecting slow-roll to NSR eras. Oftentimes, a numerical analysis is needed.

In this work, we consider large values for the slow-roll quantity $|\eta|$, and use the inverse $1/|\eta|$ as expansion parameter. A large value of $|\eta|$ is not inconceivable to obtain at the price of tunings, for example in constant roll systems. Here we are not interested in model building, but in investigating the consequences of a large $|\eta|$ limit for the dynamics of fluctuations. When working at leading order in $1/|\eta|$ formulas simplify, and we obtain analytic expressions for the two and three point functions of curvature fluctuations. These analytic results can be useful to get insights on the properties of curvature fluctuations in PBH scenarios, as well as understanding the physical consequences of a rapid growth of the curvature spectrum from large to small scales.

This idealized, large-$|\eta|$ limit has some intriguing analogy with the large-N limit of $SU(N)$ QCD, a model introduced by 't Hooft [21] in a particle physics context. N being the number of colors, the field-theory analysis can be carried on using a perturbative $1/N$ expansion, and simplifies in a large-N limit. Real world QCD has $N = 3$ colors only, yet the results of an $1/N$ expansion catch various important properties of standard QCD: we refer the reader to chapter 8 of [22] for a pedagogical survey. Calling g the QCD coupling constant, and N the number of colors, 't Hooft finds convenient to take the simultaneous limits $g \to 0$, $N \to \infty$, and gN^2 fixed [21]. Analogously, in PBH forming scenarios, it is convenient to consider the limit of vanishing e-folds of NSR expansion, $\Delta N_{\rm NSR} \to 0$, and at the same time taking $|\eta| \to \infty$, keeping fixed the product $(\Delta N_{\rm NSR}|\eta|)$. As we will learn, this product is associated with the growth of the spectrum from large to small scales. Keeping $(\Delta N_{\rm NSR}|\eta|)$ fixed, and expanding in $1/|\eta|$, the formulas for the curvature fluctuation n-point functions become easier to deal with.

[*]g.tasinato2208@gmail.com

Having analytical control on a perturbative expansion in $1/|\eta|$ allows us to address the issue of loop corrections, a topic that recently raised much attention after the important papers [23,24] appeared. As pointed out in [23], the same mechanisms that causes the curvature spectrum growth, as needed for producing PBH, also amplify the effects of loop corrections to the curvature power spectrum. Their size can become so large to invalidate a perturbative loop expansion. Many solutions and new perspectives have recently pointed out [25–36]. In the framework of a large $|\eta|$ expansion, we show that loop corrections can be placed under control, at least at the large scales that can affect CMB physics. We regularize loop integrals by means of ultraviolet and infrared cut-offs, and analytically compute the effects of loops in a large $|\eta|$ regime. The resulting ultraviolet divergences can be adsorbed into physically measurable quantities corresponding to the amplitude and the large-scale tilt of the spectrum. We are left with log-enhanced infrared contributions, whose size is small at large scales.

We hope that the tool of an $1/|\eta|$ expansion, although idealized, can lead to analytical insights allowing to further investigate properties of the dynamics of curvature fluctuations in PBH scenarios. It will be interesting to further apply this method to related topics, as the behavior of higher order n-point functions, and their corresponding loop corrections in a large $|\eta|$ limit. Having analytic expressions for the primordial correlators can also be useful for investigating the actual process of PBH formation in the postinflationary universe, as well as the generation of second-order gravitational waves from enhanced curvature spectra: see respectively e.g. [37,38] for reviews. We leave these topics to future investigations.

II. SYSTEM UNDER CONSIDERATION

We consider single field models of inflation with canonical kinetic terms. Around a conformally flat cosmological metric, $ds^2 = a^2(\tau)(-\mathrm{d}\tau^2 + d\vec{x}^2)$, the quadratic action for the curvature perturbation in Fourier space reads (we set the Planck mass to unity)

$$S_{\rm quad} = \frac{1}{2}\int d\tau d^3k z^2(\tau)[\zeta_k'^2(\tau) + k^2\zeta_k^2(\tau)], \quad (2.1)$$

where the pump field $z(\tau)$ is given by

$$z(\tau) = a(\tau)\sqrt{2\epsilon(\tau)}. \quad (2.2)$$

The definitions of Hubble and slow-roll parameters are

$$H(\tau) = \frac{a'(\tau)}{a^2(\tau)}; \qquad \epsilon(\tau) = -\frac{H'(\tau)}{a(\tau)H^2(\tau)};$$
$$\eta(\tau) = \frac{\epsilon'(\tau)}{a(\tau)H(\tau)\epsilon(\tau)}. \quad (2.3)$$

We assume that the first slow-roll parameter $\epsilon(\tau)$ remains small during the entire duration of inflation, which takes place for negative conformal time $\tau \leq \tau_0 = 0$. We also assume that the second parameter $\eta(\tau)$ remains small for negative values of τ, a part from a brief time interval $\tau_1 \leq \tau \leq \tau_2$ during which η is negative and its size $|\eta|$ becomes larger than one. (See the brief discussion in Sec. I.) During this short phase, which we call nonslow-roll (NSR) period, we cannot make a perturbative slow-roll expansion in $|\eta|$: other methods are needed to tackle the evolution of fluctuations. In this work, we explore the possibility to consider the inverse $1/|\eta|$ as a convenient expansion parameter for pursuing analytical considerations. But before discussing the role of the $|\eta|$ parameter, we first examine a quantity related with the duration of NSR phase. We build a dimensionless positive parameter $\Delta\tau$, as

$$\Delta\tau = -\frac{\tau_2 - \tau_1}{\tau_1}, \quad (2.4)$$

and we require that $\Delta\tau \ll 1$. This condition implies that the duration of the NSR phase is short with respect to the typical timescales one encounters in treating the system, as e.g. $|\tau_1|$ which controls the onset of the NSR phase. A short duration of nonslow-roll phase is demanded by the requirement to avoid excessive stochastic effects [39–41]. Since we assume that the slow-roll parameter $\epsilon(\tau)$ remains always small during inflation, we consider for simplicity the limit of pure de Sitter expansion, with $a(\tau) = -1/(H_0\tau)$ and H_0 constant during inflation. If the interval $\Delta\tau$ of Eq. (2.4) is small, this parameter has a physical interpretation in terms of a (small) number $\Delta N_{\rm NSR}$ of e-folds of NSR evolution:

$$\Delta N_{\rm NSR} = \ln\left(\frac{a(\tau_2)}{a(\tau_1)}\right) = \ln\left(\frac{\tau_1}{\tau_2}\right) = \ln\left(\frac{1}{1-\Delta\tau}\right) \simeq \Delta\tau, \quad (2.5)$$

where in the next-to-last equality we used the definition (2.4), and in the last equality we expanded for small $\Delta\tau$.

In the regime of $\Delta\tau \ll 1$ we can use the results of [42] (reviewed in the technical Appendix A): we write the solution for the mode function of the curvature perturbation $\zeta_\kappa(\tau)$ in Fourier space during different epochs in the inflationary evolution. We define the pivot scale

$$k_\star = 1/|\tau_1|, \quad (2.6)$$

corresponding to modes leaving the horizon at the onset of the NSR era. We express our formulas in terms of dimensionless momentum scales, as follows:

$$\kappa \equiv -k\tau_1 = k/k_\star. \quad (2.7)$$

Our expressions simplify with this notation, as we can easily identify modes with $\kappa \sim 1$ which cross the horizon at epochs corresponding to the NSR phase. For this reason,

we adopt from now on the dimensionless definition (2.7) when treating momenta.

The mode function $\zeta_\kappa(\tau)$ acquires its usual profile matching the Bunch-Davies vacuum at short distances:

$$\zeta_\kappa(\tau) = -i\frac{H_0(-\tau_1)^{3/2}}{\sqrt{4\epsilon_1}\kappa^{3/2}}\left(1-\frac{i\tau}{\tau_1}\right)e^{i\frac{\kappa\tau}{\tau_1}}; \quad \tau \le \tau_1 \tag{2.8}$$

for conformal times $\tau \le \tau_1$, since at early times the modes do not yet experience the NSR evolution. In the previous equation, H_0 is the constant Hubble parameter during inflation, and

$$\epsilon_1 = \epsilon(\tau_1) \tag{2.9}$$

is the value of the first slow-roll parameter at $\tau = \tau_1$.

For later times $\tau_2 \le \tau \le \tau_0$ during inflation, instead, the profile of the mode function is modified by the effects of the NSR era. See Appendix A, where we include the behavior of the mode function in the interval $\tau_1 \le \tau \le \tau_2$ that we do not need in the main text. (Sufficient to say that the mode functions, with their first derivatives, are continuous at the transition between slow-roll and nonslow-roll eras.) We find

$$\zeta_k(\tau) = -i\frac{H_0(-\tau_1)^{3/2}}{\sqrt{4\epsilon_1}\kappa^{3/2}}\left[\mathcal{C}_1(\kappa)\left(1-\frac{i\tau}{\tau_1}\right)e^{i\frac{\kappa\tau}{\tau_1}} + \mathcal{C}_2(\kappa)\left(1+\frac{i\tau}{\tau_1}\right)e^{-i\frac{\kappa\tau}{\tau_1}}\right]; \qquad \tau_2 \le \tau \le \tau_0 \tag{2.10}$$

with [recall the definition of $\Delta\tau$ in Eq. (2.4)]

$$\mathcal{C}_1(\kappa) = 1 - \frac{\eta}{8(1-\Delta\tau)^2\kappa^2} \times [1 - e^{2i\kappa\Delta\tau} - 2\kappa\Delta\tau(i - 2\kappa(1-\Delta\tau))], \tag{2.11}$$

$$\mathcal{C}_2(\kappa) = \frac{\eta e^{2i(1-\Delta\tau)\kappa}}{8(1-\Delta\tau)^2\kappa^2}[1 - 2i\kappa - e^{2i\kappa\Delta\tau}(1 - 2i\kappa(1-\Delta\tau))], \tag{2.12}$$

and

$$\eta = \lim_{\tau\to\tau_1^+}\eta(\tau). \tag{2.13}$$

From now on, the quantity η refers to the definition (2.13), i.e. the value of the time-dependent $\eta(\tau)$ evaluated at the beginning of the NSR era. Notice that in the limit of negligible $\eta \to 0$, the two mode functions (2.8) and (2.10) coincide. Instead, if $|\eta|$ is large in size, the scale dependence of the mode functions (2.8) and (2.10) differs considerably. This leads to the opportunity of increasing the size of the curvature spectrum at small scales, as required by primordial black hole production. In what comes next, we examine this possibility.

III. THE TWO-POINT FUNCTION OF CURVATURE FLUCTUATIONS

In this section we show how a suitably defined large-$|\eta|$ limit allows us to analytically capture the scale dependence of the spectrum of curvature fluctuations. Starting from the mode functions obtained in the previous section, we quantize the system starting from the quadratic action (2.1) for curvature fluctuations. See e.g. [43] for a textbook discussion. We can easily compute the two-point function $\langle\zeta_\kappa(\tau_0)\zeta^*_\kappa(\tau_0)\rangle$ of curvature perturbations evaluated at the end of inflation, $\tau = \tau_0 = 0$, and the corresponding power spectrum (recall our definition (2.7) of dimensionless scale κ)

$$\mathcal{P}_\kappa \equiv \frac{\kappa^3}{2\pi^2(-\tau_1)^3}\langle\zeta_\kappa(\tau_0)\zeta^*_\kappa(\tau_0)\rangle', \tag{3.1}$$

where a prime indicates the two-point function omitting the momentum-conserving delta functions. At very large scales, $\kappa \to 0$, one finds the usual expression

$$\mathcal{P}_0 = \lim_{\kappa\to 0}\mathcal{P}_\kappa = \frac{H_0^2}{8\pi^2\epsilon_1}, \tag{3.2}$$

with the scale of $\mathcal{P}_0$ of order 10^{-9} to match CMB normalization. Since large scale modes leave the horizon much earlier than the NSR era, they are unaffected by it. It is convenient to compute the dimensionless ratio $\Pi(\kappa)$ (see [42]) between the power spectrum (3.1) evaluated at scale κ, versus the large-scale spectrum $\mathcal{P}_0$ in Eq. (3.2). We find

$$\Pi(\kappa) \equiv \frac{\mathcal{P}_\kappa}{\lim_{\kappa\to 0}\mathcal{P}_\kappa} = |\mathcal{C}_1(\kappa) + \mathcal{C}_2(\kappa)|^2, \tag{3.3}$$

with the scale-dependent $\mathcal{C}_{1,2}(\kappa)$ given in Eqs. (2.11) and (2.12). Such ratio can be considered as a dimensionless power spectrum evaluated at the end of inflation, which singles out the overall amplitude $\mathcal{P}_0$ at large scales, and encapsulates the rich scale dependence of the spectrum evolving from large to small scales. We plot $\Pi(\kappa)$ in Fig. 1, left panel, for a representative choice of parameters capable to enhance the spectrum at small scales. Physically, the scale dependence of the spectrum is due to the brief NSR phase of inflationary evolution. The NSR era is able to excite the would-be decaying mode at superhorizon scales, which starts to actively participate to the dynamics of curvature fluctuations. See e.g. [12] for a recent review. Notice that the spectrum has a pronounced dip at intermediate scales, due to a disruptive interference between the growing and decaying modes of the curvature fluctuation at super-horizon scales. The dip is followed by a steady

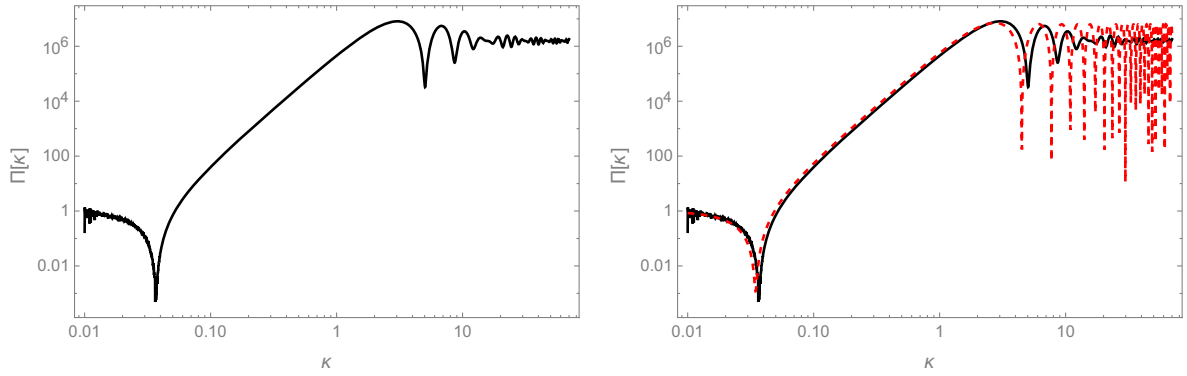

FIG. 1. Left panel: plot of the dimensionless power spectrum $\Pi(\kappa)$ as defined in Eq. (3.3): we choose the values $|\eta| = 10^4$ and $\Delta\tau = 0.2$ for the free parameters. Right panel: the black line is the same as left panel. The dashed red line represents the spectrum $\hat{\Pi}(\kappa)$ of Eq. (3.7), choosing the value $\Pi_0 = 1250$ for the single free parameter. See the discussion after Eq. (3.8). Notice that the maximal values of the spectrum occur around the onset of nonslow-roll phase, for $\kappa \sim \mathcal{O}(1)$.

growth (with slope κ^4 as first shown in [44]) until it reaches a maximal amplitude. See also [45] for a detailed analysis of the shape of the curvature power spectrum in PBH forming scenarios. We point out that—while in this work we evaluate all quantities at the end of inflation, when the inflationary dynamics ceases to affect the evolution of curvature fluctuations—the large $|\eta|$ approach can be also applied to compute correlators at any time during the inflationary era.

It is particularly interesting to evaluate the value of $\Pi(\kappa)$ at very small scales, $\kappa \to \infty$, which informs us on the total amount of the growth of the spectrum. See Fig. 1, left panel. Plugging into (3.3) the expressions for $\mathcal{C}_{1,2}$ of Eqs. (2.11) and (2.12) and taking the small-scale limit, we find

$$\lim_{\kappa\to\infty}\Pi(\kappa) = \left(\frac{1+(|\eta|/2-1)\Delta\tau}{1-\Delta\tau}\right)^2, \equiv (1+\Pi_0)^2, \tag{3.4}$$

where in the second line we introduce a constant parameter Π_0 controlling the enhancement of the spectrum from large to small scales ($\Pi_0 = 0$ means no enhancement). We would like a large enhancement of the spectrum at small scales for producing PBH. Since we are in a regime of small $\Delta\tau$, as discussed in Sec. II, we need to consider large values for the parameter $|\eta|$ during the NSR period (we make the hypothesis that η is negative, hence the absolute value). In fact, in the limit of $|\eta|$ large and $\Delta\tau$ small, expression (3.4) simplifies to

$$\Pi_0 \simeq \frac{|\eta|\Delta\tau}{2}. \tag{3.5}$$

The combination (3.5), as well as the considerations above, motivates us to take the simultaneous limits:

$$|\eta| \gg 1; \qquad \Delta\tau \ll 1; \qquad \text{keep } \Pi_0 \text{ fixed}. \tag{3.6}$$

This is reminiscent of the 't Hooft limit one encounters in particle physics [21], as explained in Sec. I. In fact, combining $|\eta|$ and $\Delta\tau$ into the fixed quantity Π_0 allows us to consistently perform expansions in the small parameter $1/|\eta|$, maintaining at the same time control on the effects of the NSR through the quantity Π_0. In most PBH scenarios we aim to a total enhancement of the order 10^6–10^7 in Eq. (3.4). Then the quantity Π_0 results by itself large, of order 10^3–10^4.

Adopting the limits of Eq. (3.6), the expression for the ratio (3.3) simplifies. We substitute $\Delta\tau = 2\Pi_0/|\eta|$ in Eq. (3.3), and expand for large values of $|\eta|$ keeping Π_0 fixed. At leading order in this expansion, we obtain

$$\hat{\Pi}(\kappa) = 1 - 4\kappa\Pi_0\cos\kappa j_1(\kappa) + 4\kappa^2\Pi_0^2 j_1^2(\kappa), \tag{3.7}$$

where a hat indicates that we only include the leading order in an expansion in $1/|\eta|$, following the conditions of Eq. (3.6). The spherical Bessel function $j_1(\kappa)$ is given by

$$j_1(\kappa) = \frac{\sin\kappa}{\kappa^2} - \frac{\cos\kappa}{\kappa}; \qquad j_1(\kappa \ll 1) = \frac{\kappa}{3} - \frac{\kappa^3}{30} + \mathcal{O}(\kappa^5). \tag{3.8}$$

We represent formula (3.7) in Fig. 1, right panel, in comparison with the result obtained by the more accurate formula (3.3). The latter, plotted in the left panel of the figure, makes use of a small $\Delta\tau$ limit only, without the further expansion in $1/|\eta|$ of Eq. (3.6). The resulting profile of the spectrum is very similar in both cases, at least in the regime $\kappa \leq 5$, indicating that the limits of Eq. (3.6) give trustable results for the spectrum at least at relatively large scales. It is not difficult to use Eq. (3.7) to analytically determine the position of the dip, finding agreement with other works in the literature [42].

It is remarkable to obtain such a simple formula (3.7) for the scale dependence of the curvature power spectrum, whose momentum profile shares features with more realistic PBH models discussed in the literature. This formula

depends on a single free parameter Π_0. Besides parametrizing the total enhancement of the spectrum, this quantity also governs the scale dependence of the spectrum at large scales. Expanding (3.7) up to κ^2:

$$\hat{\Pi}(\kappa) = 1 - \frac{4\Pi_0}{3}\kappa^2 + \mathcal{O}(\kappa^4), \tag{3.9}$$

making manifest the role of Π_0 in controlling the deviations from a flat spectrum. (See also Starobinsky's scenario [46] for a specific model leading to an interesting analytical formula for the curvature spectrum beyond slow-roll.) We can be more precise and analytically compute the spectral index associated with Eq. (3.7):

$$\hat{n}_s(\kappa) - 1 \equiv \frac{d\ln\hat{\Pi}(\kappa)}{d\ln\kappa}, \tag{3.10}$$

$$= \frac{2\kappa\Pi_0[(1-2\kappa^2)\sin(2\kappa) - 2\kappa\cos(2\kappa)]}{\kappa^2 + 4\kappa\Pi_0\cos\kappa(\kappa\cos\kappa - \sin\kappa) + 4\Pi_0^2(\kappa\cos\kappa - \sin\kappa)^2} - \frac{\Pi_0^2[4 - (4-8\kappa^2)\cos(2\kappa) + 4\kappa(\kappa^2-2)\sin(2\kappa)]}{\kappa^2 + 4\kappa\Pi_0\cos\kappa(\kappa\cos\kappa - \sin\kappa) + 4\Pi_0^2(\kappa\cos\kappa - \sin\kappa)^2}. \tag{3.11}$$

The rich dependence in momentum scale of the spectral index in Eq. (3.11) reflects the scale dependence of the spectrum in Fig. 1. We represent it in Fig. 2 for a range of momenta going from the dip position to small scales. Comparing Figs. 1 and 2, we notice that, after the dip position, the maximal growth slope of the spectrum is $n_s - 1 \leq 4$. This agrees with the more sophisticated analysis 44]] based on complete expressions for the curvature power spectrum, outside the large $|\eta|$ limit we consider here.

IV. THE THREE-POINT FUNCTION OF CURVATURE FLUCTUATIONS

We now apply the previous setup to the study of three-point function of curvature fluctuations, evaluated at the end of inflation. This quantity controls the non-Gaussianity of curvature fluctuations in PBH scenarios. We assume that the slow-roll parameter $\epsilon(\tau)$ remains always small, while $\eta(\tau)$ experiences a sharp transition between the slow-roll and non-slow-roll phases, at $\tau = \tau_1$ and $\tau = \tau_2$. The n-point functions of ζ can be computed using the in-in formalism [47–49]. Let $\mathcal{O}(\tau)$ the operator one wishes to determine (for us, the three-point function $\langle\zeta_{\kappa_1}(\tau_0)\zeta_{\kappa_2}(\tau_0)\zeta_{\kappa_3}(\tau_0)\rangle$), and $\mathcal{H}_{\rm int}$ the interaction Hamiltonian. We map the time evolution of the operator from the initial $|{\rm in}\rangle$ vacuum up to the time the operator $\mathcal{O}(\tau)$ is evaluated, and then we map back to the $|{\rm in}\rangle$ vacuum again. In formulas: $\langle{\rm in}|\bar{T}e^{-i\int\mathcal{H}_{\rm int}(\tau')d\tau'}\mathcal{O}(\tau)Te^{i\int\mathcal{H}_{\rm int}(\tau')d\tau'}|{\rm in}\rangle$. In our case, since we focus on sudden transitions, there is a single dominant contribution to the interaction Hamiltonian [23,24], which can be extracted[1] from the third-order action of perturbations in single field inflation [47]:

$$\mathcal{H}_{\rm int} = -\frac{1}{2}\int d^3x a^2(\tau)\epsilon(\tau)\eta'(\tau)\zeta^2(\tau,\vec{x})\zeta'(\tau,\vec{x}). \tag{4.1}$$

We assume that $|\eta|$ is negligible during slow-roll evolution ($\tau < \tau_1$ and $\tau_2 < \tau < \tau_0$) while it is large during the intermediate NSR phase, $\tau_1 \leq \tau \leq \tau_2$. We adopt a sharp-transition Ansatz [24] for the time-derivative of $\eta(\tau)$

$$\eta'(\tau) = \Delta\eta[-\delta(\tau-\tau_1) + \delta(\tau-\tau_2)], \tag{4.2}$$

where the times $\tau_{1,2}$ correspond to the onset and end of the NSR phase during inflation. Sudden transitions with

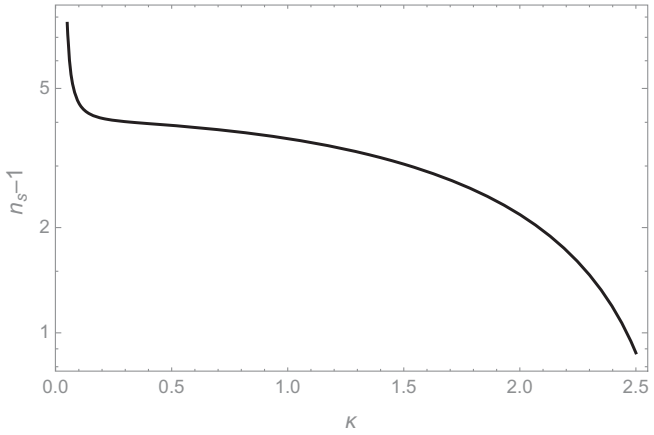

FIG. 2. The spectral index as given in Eq. (3.11), choosing $\Pi_0 = 1250$.

[1]The complete third-order Lagrangian density for scalar fluctuations in single field inflation can be found in Eq. (3.9) of the original work by Maldacena [47] (see also Eq. (35) of [24]). All terms of the Lagrangian are slow-roll suppressed, but there is a single contribution proportional to the time-derivative of η: $1/2\epsilon\eta'\zeta'\zeta^2$. This single term can give a large effect in our context with sudden transitions between slow-roll and non-slow-roll eras. As done in [23,24], we then focus on this contribution to the third order action, leading to the interaction Hamiltonian in Eq. (4.1).

jumps in the first derivatives of the inflation scalar profile and the parameter η can be explicitly realized in scenarios as the Starobinsky model [46], with a piecewise linear potential characterized by abrupt changes in its slope.

Soon we will discuss a criterium to select the constant $\Delta\eta$. But first, we apply the aforementioned in-in approach with the interaction Hamiltonian (4.1) and (4.2). The curvature three-point function, evaluated at the end of inflation $\tau_0(=0)$, results [24]

$$\langle\zeta_{\kappa_1}(\tau_0)\zeta_{\kappa_2}(\tau_0)\zeta_{\kappa_3}(\tau_0)\rangle' = -2\Delta\eta\left(\epsilon(\tau_2)a^2(\tau_2)\mathrm{Im}\left[\left(\zeta_{\kappa_1}(\tau_0)\zeta^*_{\kappa_1}(\tau_2)\right)\left(\zeta_{\kappa_2}(\tau_0)\zeta^*_{\kappa_2}(\tau_2)\right)\left(\zeta_{\kappa_3}(\tau_0)\partial_{\tau_2}\zeta^*_{\kappa_3}(\tau_2)\right)\right] - (\tau_2\to\tau_1)\right) + \text{perms}, \tag{4.3}$$

where recall that the prime means that we understand the momentum-conserving delta functions. In the squeezed limit, Eq. (4.3) reduces to

$$\lim_{\kappa_1\to 0;\kappa_2\simeq\kappa_3}\langle\zeta_{\kappa_1}(\tau_0)\zeta_{\kappa_2}(\tau_0)\zeta_{\kappa_3}(\tau_0)\rangle' = -4\Delta\eta\epsilon(\tau_2)a^2(\tau_2)|\zeta_{\kappa_1}(\tau_0)|^2|\zeta_{\kappa_2}(\tau_0)|^2\left\{\mathrm{Im}\left[\frac{\zeta^2_{\kappa_2}(\tau_0)}{|\zeta_{\kappa_2}(\tau_0)|^2}\zeta^*_{\kappa_2}(\tau_2)(\zeta'_{\kappa_2}(\tau_2))^*\right] - \frac{\epsilon(\tau_1)a^2(\tau_1)}{\epsilon(\tau_2)a^2(\tau_2)}\mathrm{Im}\left[\frac{\zeta^2_{\kappa_2}(\tau_0)}{|\zeta_{\kappa_2}(\tau_0)|^2}\zeta^*_{\kappa_2}(\tau_1)(\zeta'_{\kappa_2}(\tau_1))^*\right]\right\}. \tag{4.4}$$

The squeezed limit refers to modes with very small momenta κ_1 which leave the horizon much earlier than the onset of the non-slow-roll (NSR) phase. When selecting large-scale modes with κ_2 small, also far from the NSR epoch, we do expect that the standard Maldacena consistency relation [47] holds. Namely

$$\lim_{\kappa_1\to 0;\kappa_2\simeq\kappa_3}\langle\zeta_{\kappa_1}(\tau_0)\zeta_{\kappa_2}(\tau_0)\zeta_{\kappa_3}(\tau_0)\rangle' = -(n_s(\kappa_2)-1)|\zeta_{\kappa_1}(\tau_0)|^2|\zeta_{\kappa_2}(\tau_0)|^2. \tag{4.5}$$

We substitute our expressions for the mode functions in Eq. (2.10), and take the small κ_2 limit. Using the results of Sec. III for computing the spectral index, the two expressions (4.4) and (4.5) match once we select a certain value for the parameter $\Delta\eta$ which enters in the Ansatz (4.2). Neglecting contributions that vanish in the large-$|\eta|$ limit, we find the requirement

$$\Delta\eta = \frac{|\eta|}{(1+\Pi_0)} + \frac{\Pi_0(12+34\Pi_0+25\Pi_0^2)}{2(1+\Pi_0)^2(1+2\Pi_0)}, \tag{4.6}$$

as well as the expected condition[2]

$$\frac{\epsilon(\tau_1)a^2(\tau_1)}{\epsilon(\tau_2)a^2(\tau_2)} = 1+2\Pi_0. \tag{4.7}$$

Interestingly, although the constant $\Delta\eta$ has been fixed to satisfy Maldacena condition in the small-κ_2 limit, the resulting expression (4.4) for the squeezed three-point function that matches well with single-field Maldacena consistency relation also for larger scales: see Fig. 3, left panel, which is also in agreement with [50,51]. The resulting squeezed non-Gaussianity is strongly scale-dependent [52,53].

The squeezed limit of the three-point function, as in Eq. (4.4), is not the only interesting configuration. From the complete expression for the three-point function, Eq. (4.3), we can also consider other shapes. For example, let us consider the equilateral limit $\kappa_i = \kappa$ for $i = 1, 2, 3$. In Fig. 3, right panel, we represent the value for the three-point function as a function of the dimensionless scale κ, divided by the square of the large-scale power spectrum, Eq. (3.2) (we further divide it by Π_0^3). Namely,

$$\frac{f_{\rm eq}(\kappa)}{\Pi_0^3} \equiv \frac{\langle\zeta_\kappa(\tau_0)\zeta_\kappa(\tau_0)\zeta_\kappa(\tau_0)\rangle'}{\Pi_0^3\mathcal{P}_0^2}. \tag{4.8}$$

This quantity aims to capture the scale-dependence of the non-Gaussian equilateral limit [54], analogously to the scale-dependent part of the power spectrum of Eq. (3.2). Remarkably, the profile of the scale-dependence for the equilateral shape (changing its overall sign) is similar to the profile of the scale-dependent power spectrum: compare Fig. 1 with Fig. 3, right panel. It would be interesting to find a physical reason for this result.

The non-Gaussianity of curvature fluctuations in PBH scenarios is an important observable with several

[2]In fact, we are working in a regime of large $|\eta|$ and very small $\Delta\tau$, as dictated by relations (3.6). Hence, we obtain

$$\begin{aligned}\epsilon(\tau_1)a^2(\tau_1) &= \epsilon(\tau_2)a^2(\tau_2)\left(1+\tau_1\frac{\epsilon'(\tau_1)}{\epsilon(\tau_1)}\Delta\tau\right)\left(1+2\tau_1\frac{a'(\tau_1)}{a(\tau_1)}\Delta\tau\right),\\ &= \epsilon(\tau_2)a^2(\tau_2)(1+\tau_1 a(\tau_1)H(\tau_1)(\eta+2)\Delta\tau),\\ &= \epsilon(\tau_2)a^2(\tau_2)(1-(\eta+2)\Delta\tau),\\ &= \epsilon(\tau_2)a^2(\tau_2)(1+2\Pi_0),\end{aligned}$$

in agreement with condition (4.7).

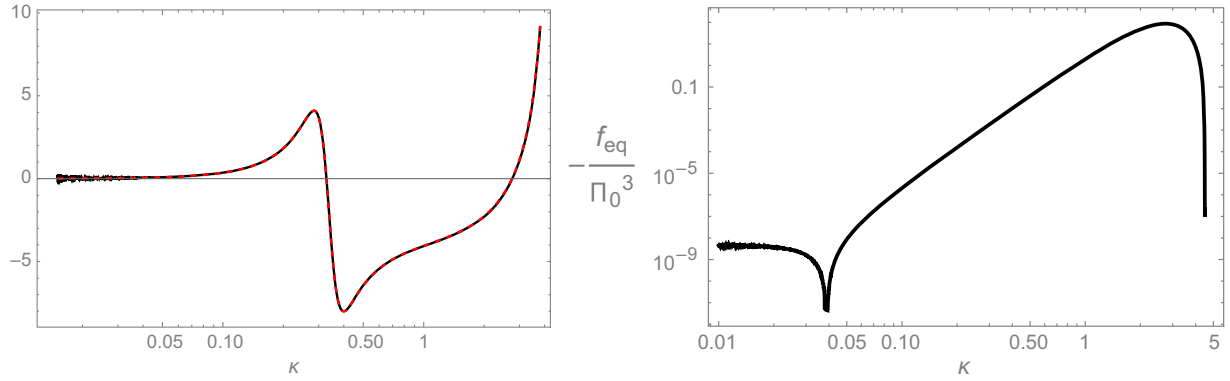

FIG. 3. Left panel: check of Maldacena consistency relation for the squeezed limit of the three point function. Black line: the quantity $1 - n_s$. Red dashed line: the squeezed limit of the three-point function of Eq. (4.4) (we omit the factors $|\zeta_{\kappa_1}(\tau_0)|^2|\zeta_{\kappa_2}(\tau_0)|^2$). We use the mode functions in Eq. (2.10), and choose the values $|\eta| = 10^{4.1}$, $\Delta\tau = 0.002$. Right panel: plot of the scale dependence of the equilateral three-point function, the quantity $-f_{\rm eq}/\Pi_0^3$, as defined in the main text, Eq. (4.8). The profile is remarkably similar to the power spectrum of Fig. 1.

phenomenological ramifications for PBH formation [55–59]. We refer the reader to [60] for a recent comprehensive analysis, and further references therein.

V. LOOP CORRECTIONS

In this section we apply the previous tools to study loop contributions to the inflationary power spectrum [61–65]. In developing our arguments, we closely follow the clear technical discussion of [24], but we make use of our large $|\eta|$ expansion, and the corresponding solutions for the mode functions discussed in Sec. II. We are especially interested in examining the physical implications of large loop corrections in our approach, and the role of the scale dependence of the spectrum. Moreover, we discuss a proposal to adsorb quadratic ultraviolet divergences into the available bare parameters in a large $|\eta|$ limit, at least at large scales relevant for CMB physics. We are left with log-enhanced, infrared effects whose size is small at large scales. This is an important step in order to clarify the relation between loops and physically measurable quantities.

The interaction Hamiltonian that we consider is given in Eq. (4.1); as in Sec. IV, we focus on a sharp transition between slow-roll regimes and an intermediate nonslow-roll regime for $\tau_1 \leq \tau \leq \tau_2$. We consider for definiteness the two-point function of curvature fluctuations in momentum space, evaluated at the scale p [dimensionless in the sense that the momentum is multiplied by $-\tau_1$, as in Eq. (2.7)]. The corresponding 1-loop contributions can be found utilizing the in-in formalism. We follow [24]: loop corrections are conveniently decomposed as

$$\langle\zeta_p(\tau_0)\zeta_p^*(\tau_0)\rangle_{\rm loop} = \langle\zeta_p(\tau_0)\zeta_p^*(\tau_0)\rangle_{(1,1)} + 2{\rm Re}\Big[\langle\zeta_p(\tau_0)\zeta_p^*(\tau_0)\rangle_{(2,0)}\Big], \tag{5.1}$$

where each term correspond to a different contribution in the expansion of the two-point correlator in the in-in formalism [24]. They read

$$\langle\zeta_p(\tau_0)\zeta_p^*(\tau_0)\rangle_{(1,1)} = \frac{1}{4}\int_{-\infty}^{\tau_0} d\tau_a a^2(\tau_a)\epsilon(\tau_a)\eta'(\tau_a)\int_{-\infty}^{\tau_0} d\tau_b a^2(\tau_b)\epsilon(\tau_b)\eta'(\tau_b)\int \Pi_{i=1}^6 \frac{d^3k_i}{(2\pi)^3}\delta^3(\vec{k}_1+\vec{k}_2+\vec{k}_3)\delta^3(\vec{k}_4+\vec{k}_5+\vec{k}_6) \times\langle\zeta'_{\vec{k}_1}(\tau_a)\zeta_{\vec{k}_2}(\tau_a)\zeta_{\vec{k}_3}(\tau_a)\zeta_{\vec{p}}(\tau_0)\zeta_{-\vec{p}}(\tau_0)\zeta'_{\vec{k}_4}(\tau_b)\zeta_{\vec{k}_5}(\tau_b)\zeta_{\vec{k}_6}(\tau_b)\rangle, \tag{5.2}$$

and

$$\langle\zeta_p(\tau_0)\zeta_p^*(\tau_0)\rangle_{(2,0)} = -\frac{1}{4}\int_{-\infty}^{\tau_0} d\tau_a a^2(\tau_a)\epsilon(\tau_a)\eta'(\tau_a)\int_{-\infty}^{\tau_0} d\tau_b a^2(\tau_b)\epsilon(\tau_b)\eta'(\tau_b)\int \Pi_{i=1}^6 \frac{d^3k_i}{(2\pi)^3}\delta^3(\vec{k}_1+\vec{k}_2+\vec{k}_3)\delta^3(\vec{k}_4+\vec{k}_5+\vec{k}_6) \times\langle\zeta_{\vec{p}}(\tau_0)\zeta_{-\vec{p}}(\tau_0)\zeta'_{\vec{k}_1}(\tau_a)\zeta_{\vec{k}_2}(\tau_a)\zeta_{\vec{k}_3}(\tau_a)\zeta'_{\vec{k}_4}(\tau_b)\zeta_{\vec{k}_5}(\tau_b)\zeta_{\vec{k}_6}(\tau_b)\rangle. \tag{5.3}$$

From now on, to simplify the calculations we focus on a large-scale regime where the size of the external momentum p is much smaller than the momenta k_i over which we integrate [23,24]. This allows to simplify formulas substituting $k - p \simeq k$, and permits us to obtain analytic results. We will discuss in due course the limitations we should impose on p for satisfying this condition, and their physical implications.

Substituting our Ansatz (4.2) in the case a sharp transition at the times τ_1 and τ_2 between slow-roll and nonslow-roll phases, the result acquires the following structure [24]

$$\begin{aligned}\langle\zeta_p(\tau_0)\zeta_p^*(\tau_0)\rangle_{\rm loop} = (2\epsilon(\tau_2)a^2(\tau_2))^2\Delta\eta^2|\zeta_{\vec{p}}(\tau_0)|^2\int\frac{d^3k}{(2\pi)^3}\Big[&|\zeta_{\vec{k}}(\tau_2)|^2{\rm Im}(\zeta_p(\tau_2)\zeta'^*_p(\tau_2)){\rm Im}(\zeta_k(\tau_2)\zeta'^*_k(\tau_2))\\ &-4\frac{\epsilon(\tau_1)a^2(\tau_1)}{\epsilon(\tau_2)a^2(\tau_2)}{\rm Im}(\zeta_p(\tau_0)\zeta_p^*(\tau_2)){\rm Im}(\zeta'_k(\tau_2)\zeta_k(\tau_2)\zeta_k^*(\tau_1)\zeta'^*_k(\tau_1))\\ &-2\frac{\epsilon(\tau_1)a^2(\tau_1)}{\epsilon(\tau_2)a^2(\tau_2)}{\rm Im}(\zeta_p(\tau_2)\zeta'^*_p(\tau_2)){\rm Im}(\zeta_k^2(\tau_2)\zeta_k^*(\tau_1)\zeta'^*_k(\tau_1))\\ &+\frac{\epsilon^2(\tau_1)a^4(\tau_1)}{\epsilon^2(\tau_2)a^4(\tau_2)}|\zeta_{\vec{k}}(\tau_1)|^2{\rm Im}(\zeta_p(\tau_1)\zeta'^*_p(\tau_1)){\rm Im}(\zeta_k(\tau_1)\zeta'^*_k(\tau_1))\Big].\end{aligned} \tag{5.4}$$

Since the integrand functions are rotationally invariant, the three-dimensional integrals over internal momenta can be decomposed into integrals over the real line as

$$\int\frac{d^3k}{(2\pi)^3}(\ldots) = \int_{\Lambda_{\rm IR}/|\eta|^{1/2}}^{\mu/|\eta|^{1/2}}\frac{k^2dk}{2\pi^2}(\ldots) + \int_{\mu/|\eta|^{1/2}}^{\Lambda_{\rm UV}/|\eta|^{1/2}}\frac{k^2dk}{2\pi^2}(\ldots) \tag{5.5}$$

with $\Lambda_{\rm IR}$ and $\Lambda_{\rm UV}$ corresponding to a very small infrared (IR) and a very large ultraviolet (UV) cutoff.[3] They are dimensionless quantities, obtained multiplying physical momentum scales with $|\tau_1|$, as in Eq. (2.7). For convenience, as a technical device we rescale the extrema of integration by $1/|\eta|^{1/2}$, to simplify our results in a large $|\eta|$ limit. The intermediate dimensionless scale μ is introduced in order to physically separate the loop corrections in an IR part [the first integral in Eq. (5.5)] and a UV part (the second integral). We can think of $\mu \sim 1$ as a scale where NSR effects take place. This separation will be essential for our arguments.

We decompose the resulting power spectrum at the end of inflation $\tau_0 = 0$ as a tree level and a loop part

$$\begin{aligned}\mathcal{P}_{\rm tot}(p) &= \frac{p^3}{2\pi^2(-\tau_1)^3}\langle\zeta_p(\tau_0)\zeta_p^*(\tau_0)\rangle\\ &= \mathcal{P}_0\hat{\Pi}(p)\Big[1 + L_{\rm loop}^{\rm IR} + L_{\rm loop}^{\rm UV}\Big],\end{aligned} \tag{5.6}$$

with $\mathcal{P}_0$ the amplitude of the large scale tree-level power spectrum as in Eq. (3.2), and $\hat{\Pi}(p)$ is the momentum-dependent function of Eq. (3.7), controlling the scale-dependent ratio between small-scale and large-scale spectra. Equation (5.6) contains the quantity $L_{\rm loop}$, the loop contribution (5.4), with the momentum integrals decomposed as in Eq. (5.5). We collect as an overall factor the momentum dependent quantity $\mathcal{P}_0\hat{\Pi}(p)$.

We substitute in the general formulas (5.5) our mode functions (2.10). We analytically perform both the IR and the UV integrals, which are much simplified in the large $|\eta|$ regime of Eq. (3.6), which keeps Π_0 fixed. At leading order in $1/|\eta|$, the dominant contribution to the IR piece of the loop correction results

$$L_{\rm loop}^{\rm IR} = -p^2\frac{\mathcal{P}_0}{3}\frac{\Pi_0^4}{(1+\Pi_0)^2(1+2\Pi_0)}\ln\left(\frac{\mu}{\Lambda_{\rm IR}}\right), \tag{5.7}$$

where we include only the log-enhanced part. Notice that the IR contribution is proportional to p^2, hence it is suppressed at large scales. As in the rest of the work, the quantity p is the dimensionless momentum scale obtained dividing the physical momentum by the pivot scale $k_\star$ [see Eq. (2.7)]. We neglect power-law quadratic pieces depending on the small quantity $\Lambda_{\rm IR}$, and on μ which, being of order one, is suppressed with respect to the logarithm in Eq. (5.7), in case of a large ratio $\mu/\Lambda_{\rm IR}$. This IR contribution can be interpreted as a secular effects caused by modes crossing the horizon from the onset of inflation until around the epoch of NSR, controlled respectively by the scales $\Lambda_{\rm IR}$ and μ. IR contributions are typically characterized by large logarithms, whose effects might contribute to observable quantities, if inflation lasts long. In our case, we can estimate $\ln(\mu/\Lambda_{\rm IR}) \sim \ln[a(\tau_1)/a(\tau_{\rm start})]$. Hence, we can expect the logarithm to be of order say 10^2. See e.g. the clear discussion in [62].

[3] From now on, our approach is a different from [23], where $\Lambda_{\rm IR,UV}$ are scales of modes leaving the horizon at the start and end of the NSR era. In our case, being the NSR epoch very short, we do not make this identification.

The dominant contribution to the UV integral is a quadratic divergence in $\Lambda_{\rm UV}$. We write the result only including the contribution quadratic in the UV cutoff

$$L^{\rm UV}_{\rm loop} = -\frac{\mathcal{P}_0\Pi_0\Lambda^2_{\rm UV}}{(1+\Pi_0)}\left(\frac{5}{6}+\frac{3j_1(p)-p}{3p}\right), \qquad (5.8)$$

and we neglect subleading contributions. As the IR contribution, also the UV part depend quadratically on a scale, this time the cut-off scale $\Lambda_{\rm UV}$. As explained after Eq. (5.5), the cutoff scales are again dimensionless quantities, obtained dividing physical cutoff scales by a pivot scale. The spherical Bessel function $j_1(p)$ defined in Eq. (3.8). The UV part contains the effects of small-scale modes, which remain in a thermal vacuum within a subhorizon regime during the first phase of inflation, until the short NSR phase occurs. These modes should not participate to the dynamics of the NSR era during inflation, and the associated UV divergences are expected to be adsorbed into appropriate, physically measurable quantities (see e.g. [66] for a detailed analysis within slow-roll models).

We adopt this viewpoint, and assume that the contributions of $L^{\rm UV}_{\rm loop}$ are adsorbed into the available parameters by means of an appropriate renormalization procedure. We discuss in Appendix B a way to do so. We are left with the log-enhanced loop contributions of Eq. (5.7). All our results are derived under the approximation stated after Eq. (5.3): to analytically compute the integrals, we make the hypothesis that the momentum p at which the two-point function (5.6) is computed is well *smaller* than the momentum scales over which integrate, i.e. the lower extremum of the integral

$$p^2 \leq \frac{\Lambda^2_{\rm IR}}{|\eta|}. \qquad (5.9)$$

Since we are working at leading order in a $1/|\eta|$ expansion, the previous condition informs us that we should only focus on the very first terms in a momentum expansion of our formulas. Using the expression (3.7), we consider Eq. (5.6) up to second order in an expansion in momentum p, including the IR loop contributions:

$$\mathcal{P}_{\rm tot}(p) = \mathcal{P}_0 - \frac{4\mathcal{P}_0\Pi_0}{3}\left[1+\frac{\mathcal{P}_0}{4}\frac{\Pi_0^3}{(1+\Pi_0)^2(1+2\Pi_0)} \times \ln\left(\frac{\mu}{\Lambda_{\rm IR}}\right)\right]p^2 + \mathcal{O}(p^4). \qquad (5.10)$$

Hence, the log-enhanced IR loop only gives a contribution to the quadratic term in the expansion. Its size is small, being suppressed by a factor $\mathcal{P}_0 \simeq 10^{-9}$ with respect to the tree level term, so even a large logarithm is unable to give large effects. The coefficients depending on Π_0 give order one effects, in the limit of Π_0 large.

We conclude this section with a comparison between our results and some recent papers appeared in the literature on this subject. The works [23,24] focus on the ultra-slow-roll case $|\eta| = 6$, assuming sudden transitions between slow-roll and nonslow-roll epochs. In this specific case, loop corrections give dangerously large contributions to correlators evaluated at large, CMB scales. Recently, the works [31,36] shown that for different values of $|\eta|$ in the nonslow-roll epoch loop corrections can be reduced, and do not necessarily spoil CMB predictions. Our large $|\eta|$ approach lies on this category of scenarios: it explores systems with $|\eta| \neq 6$, confirming that regions in parameter space with $|\eta| \gg 6$ lead to loop corrections suppressed by powers of momentum p [see Eq. (5.10)], negligible at large scales. Another possibility to explore is relaxing the assumption of sudden transition between slow-roll and ultraslow-roll phases. This idea has been carried on in [28,30,33], showing that loop effects can be considerably reduced when adopting a smooth transition between different epochs. The same remains true including higher order effects associated with quartic interactions [30]. It would be very interesting to further explore these topics in the context of our large $|\eta|$ approach, also studying the effects of loops at large values of momenta (as done for example in [36]), and carrying on a renormalization procedure using for example the techniques pursued by [32] in a related context. Moreover, it would be interesting to study higher loops, and consequences of higher order interactions making use of a large $|\eta|$ expansion. We leave these investigations for future works.

ACKNOWLEDGMENTS

It is a pleasure to thank Maria Mylova, Ogan Özsoy, and Ivonne Zavala for useful input. G. T. is partially funded by the STFC Grant No. ST/T000813/1.

APPENDIX A: CURVATURE PERTURBATIONS AND THE NSR REGIME

In this technical appendix, we briefly review the results developed in [42] to determine analytic solutions for inflationary mode functions during nonslow-roll regimes, referring the reader to [42] for more details. Starting from the quadratic action (2.1) of curvature perturbations, it is convenient to introduce a Mukhanov-Sasaki variable $v_k(\tau) = \zeta_k(\tau)/z(\tau)$, satisfying the equation

$$v_k''(\tau) + \left[k^2 - \frac{z''(\tau)}{z(\tau)}\right]v_k(\tau) = 0, \qquad (A1)$$

in momentum space. In our case, the inflationary evolution for $\tau \leq \tau_0$ undergoes different phases. We have an initial slow-roll phase for $\tau \leq \tau_1$, where both the slow-roll parameters $\epsilon(\tau)$ and $\eta(\tau)$ are very small. We can approximate this as pure de Sitter phase. Then, for $\tau_1 \leq \tau \leq \tau_2$ we

have nonslow-roll evolution where $\epsilon(\tau)$ keeps small, while $\eta(\tau)$ is negative but potentially large in size. We denote with ϵ_1 and η the values of the slow-roll parameters evaluated at $\tau \to \tau_1^+$. Finally, a slow-roll phase $\tau_2 < \tau \leq \tau_0$ where the slow-roll parameters return to very small values. Again, we approximate this last phase to pure de Sitter. We assume that the pump field $z(\tau)$ is continuous at the transitions.

In the de Sitter limit, while $z''(\tau)/z(\tau) = 2/\tau^2$ for $\tau \leq \tau_1$ and $\tau_2 < \tau \leq \tau_0$, the time-profile for this quantity can be richer. As in [42], we adopt an Ansatz

$$v_k(\tau) = -\frac{iH_0 z(\tau) e^{-ik\tau}}{2\sqrt{\epsilon_1 k^3}} \mathcal{C}_1(k)[1 + ik\tau + (ik\tau_1)^2 A_{(2)}(\tau) + (ik\tau_1)^3 A_{(3)}(\tau)] - \frac{iH_0 z(\tau) e^{ik\tau}}{2\sqrt{\epsilon_1 k^3}} \mathcal{C}_2(k)[1 - ik\tau + (-ik\tau_1)^2 A_{(2)}(\tau) + (-ik\tau_1)^3 A_{(3)}(\tau)] \tag{A2}$$

for the Mukhanov-Sasaki mode function.

For $\tau < \tau_1$, the mode equation is the same as in a standard slow-roll era: in order to match with the Bunch-Davies vacuum, we select $A_{(n)} = 0$ for $n \geq 2$, as well as $\mathcal{C}_2 = 0$ and $\mathcal{C}_1 = 1$ in Eq. (A2). For $\tau_1 \leq \tau \leq \tau_2$, we can use the Ansatz (A2) in the evolution equation (A1), and solve the equation order by order in powers of $(k\tau_1)$: see [42]. At each order n in $(k\tau_1)^n$, the equation can be solved at leading order in an expansion in the parameter $\Delta\tau$ of Eq. (2.4) controlling the duration of the non-slow-roll era. For each n, the result depends on powers of the quantity $d\ln[z^2(\tau)/a^2(\tau)]/d\ln\tau$, evaluated at time τ_1^+ at the onset of the NSR era. This quantity was dubbed α in [42]: in the present instance, within single field inflation with canonical kinetic terms and in a pure de Sitter limit, it corresponds to the quantity $-\eta$ [we use the definitions (2.3)]. After computing each quantity $A_{(n)}$, the resulting series in Eq. (A2) can be resummed analytically in terms of exponentials. The result of the resummation is [42]

$$v_k(\tau) = -\frac{iH_0 z(\tau) e^{-ik\tau}}{2\sqrt{\epsilon_1 k^3}} \left[1 + ik\tau + \frac{\eta}{4}(1 - 2ik(\tau - \tau_1) - e^{2ik(\tau-\tau_1)})\right], \tag{A3}$$

valid for $\tau_1 \leq \tau \leq \tau_2$. This mode function continuously connects, together with its first derivative, with the mode function (and the Bunch-Davies vacuum) for $\tau \leq \tau_1$. We can finally connect the result of Eq. (A3) with de Sitter mode function at later times $\tau_2 \leq \tau \leq \tau_0$, imposing continuity of the function and its first derivative at $\tau = \tau_2$. The solution corresponds to Ansatz (A2) with $A_{(n)} = 0$, and the scale-dependent functions $\mathcal{C}_1$ and $\mathcal{C}_2$ are collected in Eqs. (2.11) and (2.12) of the main text.

APPENDIX B: RENORMALIZATION OF UV DIVERGENCES

In this appendix we briefly discuss a method for adsorbing the UV quadratically-divergent parts (5.8) of the loop contributions into the available parameters of the system, at least at large scales for $p \ll 1$. The quantities available for this procedure are the overall amplitude $\mathcal{P}_0$ defined in Eq. (3.2), and the factor Π_0 controlling the scale-dependence of the tree level spectrum (3.7). As stated in the main text, we can trust our results only on a large-scale, small-p regime. [See discussion around Eq. (5.9).] Expanding the total power spectrum (5.6) up to quadratic order in p, and including the UV one-loop contributions given in Eq. (5.8), we obtain:

$$\mathcal{P}_{\rm tot}(p) = \mathcal{P}_0\left(1 - \frac{5\Pi_0\Lambda_{\rm UV}^2\mathcal{P}_0}{6(1+\Pi_0)}\right) - \frac{4\mathcal{P}_0\Pi_0}{3}\left(1 - \frac{103\Lambda_{\rm UV}^2\mathcal{P}_0}{120(1+\Pi_0)}\right)p^2 + \mathcal{O}(p^4). \tag{B1}$$

The parenthesis contain the UV-divergent loop contributions, suppressed by a factor $\mathcal{P}_0$ with respect to the tree-level terms. Higher loop corrections give contributions to Eq. (B1) with powers higher than two in $\mathcal{P}_0$. In the present one-loop instance, we can trust our results only up to quadratic contributions $\mathcal{P}_0^2$. We can then adsorb the UV-divergent parts of Eq. (B1) into a redefinition of the bare quantities $\mathcal{P}_0$ and Π_0, which are mapped into measurable quantities $\mathcal{P}_{\rm ms}$ and $\Pi_{\rm ms}$ at large scales:

$$\mathcal{P}_0 \to \mathcal{P}_{\rm ms}\left(1 + \frac{5\Lambda_{\rm UV}^2\Pi_{\rm ms}}{6(1+\Pi_{\rm ms})}\mathcal{P}_{\rm ms}\right), \tag{B2}$$

$$\Pi_0 \to \Pi_{\rm ms}\left(1 + \frac{\Lambda_{\rm UV}^2(103 - 100\Pi_{\rm ms})}{120(1+\Pi_{\rm ms})}\mathcal{P}_{\rm ms}\right). \tag{B3}$$

By means of this definition, we express Eq. (B1) as

$$\mathcal{P}_{\rm tot}(p) = \mathcal{P}_{\rm ms} - \frac{4\mathcal{P}_{\rm ms}}{3}\Pi_{\rm ms}p^2 + \mathcal{O}(p^4) + \mathcal{O}(\mathcal{P}_{\rm ms}^2). \tag{B4}$$

Hence quadratically divergent, one-loop effects get adsorbed into bare quantities. The result is expressed in terms of the measurable amplitude $\mathcal{P}_{\rm ms}$ of the spectrum, and on the parameter $\Pi_{\rm ms}$ controlling its scale dependence at very large scales [see the discussion around Eq. (3.9)].

It is also interesting to provide a feeling on the size of the quadratic loop corrections, by substituting representative values of the measurable parameters in Eqs. (B2) and (B3). At very large scales, we can fix the dimensionless power spectrum $\mathcal{P}_{\rm ms}$ to the value $\mathcal{P}_{\rm ms} \simeq 10^{-9}$, so to match the normalization of CMB spectrum. Moreover, if we wish to get an enhancement at least of order 10^6 in the size of the primordial spectrum from large toward small scales—in order for producing primordial black holes—we select the ratio $\Pi_{\rm ms} = 10^3$ [see Eq. (3.4)]. Equations (B2) and (B3) become

$$\mathcal{P}_0 \simeq \mathcal{P}_{\rm ms}\left(1 + \frac{5\times 10^{-9}}{6}\Lambda_{\rm UV}^2\right), \tag{B5}$$

$$\Pi_0 \simeq \Pi_{\rm ms}\left(1 - \frac{5\times 10^{-9}}{6}\Lambda_{\rm UV}^2\right). \tag{B6}$$

As explained in the main text—see comments after Eq. (5.5)—the quantity $\Lambda_{\rm UV}$ is dimensionless, being the ratio of the cutoff scale versus the pivot scale $k_\star$ of Eq. (2.6) characterizing the modes leaving the horizon during the NSR era. Hence bare and measurable quantities are of comparable size, unless the scale of the cutoff is very large (by a factor at least of order 10^4–10^5) with respect to the pivot scale.

[1] G. Bertone and D. Hooper, History of dark matter, Rev. Mod. Phys. **90**, 045002 (2018).
[2] S. Hawking, Gravitationally collapsed objects of very low mass, Mon. Not. R. Astron. Soc. **152**, 75 (1971).
[3] B. J. Carr and S. W. Hawking, Black holes in the early Universe, Mon. Not. R. Astron. Soc. **168**, 399 (1974).
[4] P. Ivanov, P. Naselsky, and I. Novikov, Inflation and primordial black holes as dark matter, Phys. Rev. D **50**, 7173 (1994).
[5] J. Garcia-Bellido, A. D. Linde, and D. Wands, Density perturbations and black hole formation in hybrid inflation, Phys. Rev. D **54**, 6040 (1996).
[6] M. Y. Khlopov, Primordial black holes, Res. Astron. Astrophys. **10**, 495 (2010).
[7] J. García-Bellido, Massive primordial black holes as dark matter and their detection with gravitational waves, J. Phys. Conf. Ser. **840**, 012032 (2017).
[8] M. Sasaki, T. Suyama, T. Tanaka, and S. Yokoyama, Primordial black holes—perspectives in gravitational wave astronomy, Classical Quantum Gravity **35**, 063001 (2018).
[9] B. Carr and F. Kuhnel, Primordial black holes as dark matter: Recent developments, Annu. Rev. Nucl. Part. Sci. **70**, 355 (2020).
[10] A. M. Green and B. J. Kavanagh, Primordial black holes as a dark matter candidate, J. Phys. G **48**, 043001 (2021).
[11] A. Escrivà, F. Kuhnel, and Y. Tada, Primordial black holes, arXiv:2211.05767.
[12] O. Özsoy and G. Tasinato, Inflation and primordial black holes, Universe **9**, 203 (2023).
[13] H. Motohashi and W. Hu, Primordial black holes and slow-roll violation, Phys. Rev. D **96**, 063503 (2017).
[14] W. H. Kinney, Horizon crossing and inflation with large η, Phys. Rev. D **72**, 023515 (2005).
[15] J. Martin, H. Motohashi, and T. Suyama, Ultra slow-roll inflation and the non-Gaussianity consistency relation, Phys. Rev. D **87**, 023514 (2013).
[16] K. Dimopoulos, Ultra slow-roll inflation demystified, Phys. Lett. B **775**, 262 (2017).
[17] H. Motohashi, A. A. Starobinsky, and J. Yokoyama, Inflation with a constant rate of roll, J. Cosmol. Astropart. Phys. 09 (2015) 018.
[18] S. Inoue and J. Yokoyama, Curvature perturbation at the local extremum of the inflaton's potential, Phys. Lett. B **524**, 15 (2002).
[19] K. Tzirakis and W. H. Kinney, Inflation over the hill, Phys. Rev. D **75**, 123510 (2007).
[20] D. Wands, Duality invariance of cosmological perturbation spectra, Phys. Rev. D **60**, 023507 (1999).
[21] G. 't Hooft, A planar diagram theory for strong interactions, Nucl. Phys. **B72**, 461 (1974).
[22] S. Coleman, *Aspects of Symmetry: Selected Erice Lectures* (Cambridge University Press, Cambridge, England, 1985).
[23] J. Kristiano and J. Yokoyama, Ruling out primordial black hole formation from single-field inflation, arXiv:2211.03395.
[24] J. Kristiano and J. Yokoyama, Response to criticism on ruling out primordial black hole formation from single-field inflation: A note on bispectrum and one-loop correction in single-field inflation with primordial black hole formation, arXiv:2303.00341.
[25] A. Riotto, The primordial black hole formation from single-field inflation is not ruled out, arXiv:2301.00599.
[26] S. Choudhury, M. R. Gangopadhyay, and M. Sami, No-go for the formation of heavy mass primordial black holes in single field inflation, arXiv:2301.10000.
[27] S. Choudhury, S. Panda, and M. Sami, No-go for PBH formation in EFT of single field inflation, arXiv:2302.05655.
[28] A. Riotto, The primordial black hole formation from single-field inflation is still not ruled out, arXiv:2303.01727.
[29] S. Choudhury, S. Panda, and M. Sami, Quantum loop effects on the power spectrum and constraints on primordial black holes, arXiv:2303.06066.
[30] H. Firouzjahi, One-loop corrections in power spectrum in single field inflation, arXiv:2303.12025.

[31] H. Motohashi and Y. Tada, Squeezed bispectrum and one-loop corrections in transient constant-roll inflation, arXiv:2303.16035.
[32] S. Choudhury, S. Panda, and M. Sami, Galileon inflation evades the no-go for PBH formation in the single-field framework, arXiv:2304.04065.
[33] H. Firouzjahi and A. Riotto, Primordial black holes and loops in single-field inflation, arXiv:2304.07801.
[34] E. Tomberg, Stochastic constant-roll inflation and primordial black holes, Phys. Rev. D **108**, 043502 (2023).
[35] H. Firouzjahi, Loop corrections in gravitational wave spectrum in single field inflation, arXiv:2305.01527.
[36] G. Franciolini, A. Iovino, Jr., M. Taoso, and A. Urbano, One loop to rule them all: Perturbativity in the presence of ultra slow-roll dynamics, arXiv:2305.03491.
[37] A. Escrivà, PBH formation from spherically symmetric hydrodynamical perturbations: A review, Universe **8**, 66 (2022).
[38] G. Domènech, Scalar induced gravitational waves review, Universe **7**, 398 (2021).
[39] C. Pattison, V. Vennin, H. Assadullahi, and D. Wands, Quantum diffusion during inflation and primordial black holes, J. Cosmol. Astropart. Phys. 10 (2017) 046.
[40] J. M. Ezquiaga, J. García-Bellido, and V. Vennin, The exponential tail of inflationary fluctuations: Consequences for primordial black holes, J. Cosmol. Astropart. Phys. 03 (2020) 029.
[41] D. G. Figueroa, S. Raatikainen, S. Rasanen, and E. Tomberg, Implications of stochastic effects for primordial black hole production in ultra-slow-roll inflation, J. Cosmol. Astropart. Phys. 05 (2022) 027.
[42] G. Tasinato, An analytic approach to non-slow-roll inflation, Phys. Rev. D **103**, 023535 (2021).
[43] A. R. Liddle and D. H. Lyth, Cosmological inflation and large scale structure (2000).
[44] C. T. Byrnes, P. S. Cole, and S. P. Patil, Steepest growth of the power spectrum and primordial black holes, J. Cosmol. Astropart. Phys. 06 (2019) 028.
[45] O. Özsoy and G. Tasinato, On the slope of the curvature power spectrum in non-attractor inflation, J. Cosmol. Astropart. Phys. 04 (2020) 048.
[46] A. A. Starobinsky, Spectrum of adiabatic perturbations in the universe when there are singularities in the inflation potential, JETP Lett. **55**, 489 (1992).
[47] J. M. Maldacena, Non-Gaussian features of primordial fluctuations in single field inflationary models, J. High Energy Phys. 05 (2003) 013.
[48] X. Chen, M.-x. Huang, S. Kachru, and G. Shiu, Observational signatures and non-Gaussianities of general single field inflation, J. Cosmol. Astropart. Phys. 01 (2007) 002.
[49] D. Seery and J. E. Lidsey, Primordial non-Gaussianities in single field inflation, J. Cosmol. Astropart. Phys. 06 (2005) 003.
[50] O. Özsoy and G. Tasinato, CMB μT cross correlations as a probe of primordial black hole scenarios, Phys. Rev. D **104**, 043526 (2021).
[51] O. Özsoy and G. Tasinato, Consistency conditions and primordial black holes in single field inflation, Phys. Rev. D **105**, 023524 (2022).
[52] C. T. Byrnes, S. Nurmi, G. Tasinato, and D. Wands, Scale dependence of local fNL, J. Cosmol. Astropart. Phys. 02 (2010) 034.
[53] C. T. Byrnes, M. Gerstenlauer, S. Nurmi, G. Tasinato, and D. Wands, Scale-dependent non-Gaussianity probes inflationary physics, J. Cosmol. Astropart. Phys. 10 (2010) 004.
[54] X. Chen, Running non-Gaussianities in DBI inflation, Phys. Rev. D **72**, 123518 (2005).
[55] C. T. Byrnes, E. J. Copeland, and A. M. Green, Primordial black holes as a tool for constraining non-Gaussianity, Phys. Rev. D **86**, 043512 (2012).
[56] S. Young and C. T. Byrnes, Primordial black holes in non-Gaussian regimes, J. Cosmol. Astropart. Phys. 08 (2013) 052.
[57] S. Passaglia, W. Hu, and H. Motohashi, Primordial black holes and local non-Gaussianity in canonical inflation, Phys. Rev. D **99**, 043536 (2019).
[58] M. Biagetti, V. De Luca, G. Franciolini, A. Kehagias, and A. Riotto, The formation probability of primordial black holes, Phys. Lett. B **820**, 136602 (2021).
[59] V. Atal and C. Germani, The role of non-Gaussianities in primordial black hole formation, Phys. Dark Universe **24**, 100275 (2019).
[60] M. Taoso and A. Urbano, Non-Gaussianities for primordial black hole formation, J. Cosmol. Astropart. Phys. 08 (2021) 016.
[61] S. Weinberg, Quantum contributions to cosmological correlations, Phys. Rev. D **72**, 043514 (2005).
[62] M. S. Sloth, On the one loop corrections to inflation and the CMB anisotropies, Nucl. Phys. **B748**, 149 (2006).
[63] D. Seery, One-loop corrections to the curvature perturbation from inflation, J. Cosmol. Astropart. Phys. 02 (2008) 006.
[64] L. Senatore and M. Zaldarriaga, On loops in inflation, J. High Energy Phys. 12 (2010) 008.
[65] N. Bartolo, E. Dimastrogiovanni, and A. Vallinotto, One-loop corrections to the power spectrum in general single-field inflation, J. Cosmol. Astropart. Phys. 11 (2010) 003.
[66] D. Boyanovsky, H. J. de Vega, and N. G. Sanchez, Quantum corrections to slow roll inflation and new scaling of superhorizon fluctuations, Nucl. Phys. **B747**, 25 (2006).